Published in final edited form as:
Am J Physiol Renal Physiol. 2008 March ; 294(3): F562–F570. doi:10.1152/ajprenal.00387.2007.

20-HETE-mediated cytotoxicity and apoptosis in ischemic kidney epithelial cells

Vani Nilakantan[1,4], **Cheryl Maenpaa**[1,4], **Guangfu Jia**[2,4], **Richard J. Roman**[3,4], and **Frank Park**[2,3,4]

[1]Department of Transplant Surgery, Medical College of Wisconsin Milwaukee, Wisconsin

[2]Department of Medicine, Medical College of Wisconsin Milwaukee, Wisconsin

[3]Department of Physiology, Medical College of Wisconsin Milwaukee, Wisconsin

[4]Kidney Disease Center, Medical College of Wisconsin Milwaukee, Wisconsin

Abstract

20-HETE, a metabolite of arachidonic acid, has been implicated as a mediator of free radical formation and tissue death following ischemia- reperfusion (IR) injury in the brain and heart. The present study examined the role of this pathway in a simulated IR renal injury model in vitro. Modified self-inactivating lentiviral vectors were generated to stably overexpress murine Cyp4a12 following transduction into LLC-PK_1 cells (LLC-Cyp4a12). We compared the survival of control and transduced LLC-PK_1 cells following 4 h of ATP depletion and 2 h of recovery in serum-free medium. ATP depletion-recovery of LLC-Cyp4a12 cells resulted in a significantly higher LDH release ($P < 0.05$) compared with LLC-enhanced green fluorescent protein (EGFP) cells. Treatment with the SOD mimetic MnTMPyP (100 μM) resulted in decreased cytotoxicity in LLC-Cyp4a12 cells. The selective 20-HETE inhibitor HET-0016 (10 μM) also inhibited cytotoxicity significantly ($P < 0.05$) in LLC-Cyp4a12 cells. Dihydroethidium fluorescence showed that superoxide levels were increased to the same degree in LLC-EGFP and LLC-Cyp4a12 cells after ATP depletion-recovery compared with control cells and that this increase was inhibited by MnTMPyP. There was a significant increase ($P < 0.05$) of caspase-3 cleavage, an effector protease of the apoptotic pathway, in the LLC-Cyp4a12 vs. LLC-EGFP cells ($P < 0.05$). This was abolished in the presence of HET-0016 ($P < 0.05$) or MnTMPyP ($P < 0.01$). These results demonstrate that 20-HETE overexpression can significantly exacerbate the cellular damage that is associated with renal IR injury and that the programmed cell death is mediated by activation of caspase-3 and is partially dependent on enhanced CYP4A generation of free radicals.

Keywords

apoptosis; cytochrome *P*-450 4A10; cytochrome *P*-450 4A12; LLC-PK_1; lentiviral vectors; kidney; HET-0016; superoxide; $O_2^{\bullet-}$

Ischemia-reperfusion (ir)-induced cell injury of polarized renal epithelial cells results in severe biochemical, physiological, and morphological alterations (15,23,41), including decreased levels of ATP, increased levels of calcium, increased reactive oxygen and

Addresses for reprint requests and other correspondence: F. Park, Depts. of Medicine and Physiology, Medical College of Wisconsin, 8701 Watertown Plank Rd., MRC 4100, Milwaukee, WI 53226 (e-mail: fpark@mcw.edu) or V. Nilakantan, Div. of Transplant Surgery, Medical College of Wisconsin, 8701 Watertown Plank Rd., MRC 4100, Milwaukee, WI 53226 (e-mail: vnilakan@mcw.edu).

oxidative stress, membrane lipid peroxidation, and changes in enzyme activities. The extent of the injury to the tubular epithelial cells is dependent on the length and severity of the ischemic period (16). At the present time, the mechanism(s) by which the renal epithelial cells are injured and programmed toward cell death following oxidative stress remains to be fully elucidated, but there are several reports on the brain and heart indicating that the cytochrome *P*-450 (CYP) enzyme family may be involved (29,39).

Cytochrome *P*-450s (CYP450) metabolize arachidonic acid into HETEs and EETs. 20-HETE, which is the ω-hydroxylation product of arachidonic acid, is one of the major CYP eicosanoids produced in the renal vasculature and tubules (9–12). The predominant P450 in the kidney that synthesizes 20-HETE in the renal epithelial cells is the P450 of the 4A (Cyp4a) family (10,37). 20-HETE is a potent vasoconstrictor and plays an important role in maintaining normal renal homeostatic function by controlling preglomerular vascular tone (21,42) as well as regulating sodium reabsorption in the proximal tubules and thick ascending loop of Henle (13,34). Alterations in the production of 20-HETE have been observed in ischemic cerebrovascular diseases, chronic kidney diseases, angiogenesis, and hypertension (21,22). In addition, inhibition of 20-HETE has been demonstrated to greatly reduce infarct size following IR injury in the brain and heart (22,28,38). The mechanism(s) by which 20-HETE contributes to reperfusion injury in the brain and heart has not been explored in previous studies. Theoretically, 20-HETE may increase infarct size by decreasing blood flow to the affected area by limiting compensatory vasodilation in the collateral circulation. Alternatively, release of 20-HETE may directly damage ischemic tissue by increasing the formation of reactive oxygen species.

In the kidney, there remains a paucity of information with regard to the role of 20-HETE during IR injury. However, there are a number of diseases originating from renal dysfunction that have been associated with pathological changes in 20-HETE production, including cyclosporine-induced nephrotoxicity (35) and altered pressure-natriuresis, leading to systemic hypertension (24). Moreover, recent work by Ward et al. (44) found that elevated urinary 20-HETE excretion was associated with increased oxidative stress in hypertensive subjects. Recently, it has been indicated that 20-HETE increases radical formation in endothelial cells in part by disassociating endothelial nitric oxide synthase (eNOS) from heat shock protein 90, leading to NOS uncoupling and increased radical formation (1). Since elevated free radical production has been previously shown to be promote renal epithelial cell damage during IR injury (2), the present study explored the potential interaction of 20-HETE and superoxide formation in an in vitro model of simulated IR injury.

To accomplish this goal, we utilized a well-studied model of IR injury in a porcine proximal tubule cell line, LLC-PK_1 (14,40). These cells were transduced using vesicular stomatitis virus G (VSV-G) pseudotyped self-inactivating lentiviral vectors overexpressing the murine Cyp4a12 isoform to increase the production of 20-HETE. Experiments were designed to assess the effects of CYP4A overexpression on cytotoxicity, superoxide levels, and apoptosis in LLC-PK_1 cells following ATP depletion-recovery.

METHODS

Reagents

Manganese (III) tetrakis (1-methyl-4-pyridyl) prophyrin pentachloride (MnTMPyP) was purchased from Axxora (San Diego, CA). *N*-hydroxy-*N*′-(4-butyl-2-methylphenol) formamidine (HET-0016) was generously provided to Dr. Richard J. Roman (Taisho Pharmaceutical, Tokyo, Japan). Hexadimethrine bromide (polybrene) was purchased from Sigma-Aldrich (St. Louis, MO).

Construction of CYP4A-expressing lentiviral vector transfer plasmid

Murine full-length Cyp4a10 (cDNA clone MGC:58977) and Cyp4a12 (cDNA clone MGC: 25972) cDNA clones were purchased from American Type Culture Collection (Manassas, VA). The Cyp4a10-expressing transfer plasmid was cloned by double digesting pHR(+)c.Ub.GFP.R(−)W(+) with *Kpn*I and *Xba*I to remove the green fluorescent protein (GFP) cDNA and replace it with the *Xba*I/*Kpn*I fragment containing the Cyp4a10 and Cyp4a12 cDNA clones. The final construct was pHR(+)c.Ub.CYP4A10.R(−)W(+). For the Cyp4a12-expressing transfer plasmid, an additional *Xba*I/*Xba*I fragment containing the 3′-end of the Cyp4a12 cDNA was cloned into the *Xba*I-digested pHR(+)c.Ub.CYP4A12(short).R(−)W(+) plasmid to make the final construct, pHR(+)c.Ub.CYP4A12.R(−)W(+).

Packaging and envelope pseudotype plasmids

pCMVΔR8.74 is the packaging plasmid that provides the expression of the *gag-pol*, *tat*, and *rev* genes, and the viral accessory genes have been deleted or attenuated as previously described by Dull et al. (5). pMD.G is the envelope plasmid and encodes VSV-G protein as previously described (25).

Lentiviral vector production

VSV-G pseudotyped SIN lentiviral vectors were produced by transient triple-plasmid transfection of 293T cells as previously described in our laboratory (30–33). In brief, the following amounts of plasmid DNA were used in the transfection protocol: 10 μg transfer plasmid, 6.5 μg packaging plasmid, and 3.5 μg envelope plasmid. Conditioned media were collected at 48 h, filtered, and frozen at −80°C. Single-channel FACS analysis (Becton-Dickinson, Franklin Lakes, NJ) was performed on EGFP-expressing lentiviral vectors and analyzed with the CellQuest program (Version 3.1f; Becton-Dickinson) to determine lentiviral vector titer. In addition, real-time PCR was performed on genomic DNA isolated from transduced HeLa cells using previously described primers targeted to the woodchuck postregulatory element (33) to determine lentiviral vector genome copy numbers.

Cell culture and vector transduction

LLC-PK_1 (a porcine proximal tubular epithelial cell line) was obtained from the American Type Culture Collection (Rockville, MD) and grown using α-MEM supplemented with glutamine, 10% fetal calf serum (Invitrogen, Carlsbad, CA), penicillin, and streptomycin. The cells were serially transduced with VSV-G pseudotyped lentiviral vectors expressing either EGFP, Cyp4a10, or Cyp4a12 in the presence of polybrene (8 μg/ml) on a daily basis, and the cells were expanded. The cells transduced with EGFP, Cyp4a10, and Cyp4a12 were labeled as LLC-EGFP, LLC-Cyp4a10, and LLC-Cyp4a12, respectively. The transduction efficiency by the lentiviral vectors was determined using FACS analysis using the LLC-EGFP cells. LLC-Cyp4a10 and LLCCyp4a12 cells were used to assess the mRNA and functional activity of the P4504A isoforms by RT-real-time PCR and the P450 enzyme assay using liquid chromatography coupled to mass spectroscopy, respectively.

RT-quantitative PCR for Cyp4a10 and Cyp4a12

Total RNA was extracted from the vehicle (LLC-VEH) and lentiviral vector-transduced LLC-PK_1 cells (LLC-EGFP, LLC-Cyp4a10, and LLC-Cyp4a12) using TRIzol reagent (Invitrogen, Carlsbad, CA). The total RNA (2 μg) was DNAse treated with 1 U of RQ1 RNAse-free DNAse (Promega, Madison, WI) for 30 min, and the RNA was reverse transcribed using oligo-dT primer and SuperScript III RTase (Invitrogen) for 60 min at 42°C. Following cDNA synthesis, the RT products was heated to 85°C for 10 min and immediately placed on ice. All primers for PCR were purchased from Integrated DNA

Technologies (Coralville, IA) using gene-specific primers for Cyp4a10 and Cyp4a12 as follows: Cyp4a10: sense 5′-GACAAGGACCTACGTGCTGAG G-3′, antisense 5′-CTCATAGCAAATTGTTTCCCA-3′; and Cyp4a12: sense 5′-TGAGTCCT ATGAAAGAGTGCC-3′, antisense 5′-CTGGAAGCCCAGCAGAAGGTG-3′. Real-time quantitative PCR was carried out with the Stratagene 3000XP real-time PCR machine using SYBR green reagents. The PCR mixture contains 1× SYBR green PCR master mix, 100 nM forward and reverse primers, and 10 ng cDNA, in a total reaction volume of 20 μl. Each reaction was performed in quadruplicate at the following conditions: 95°C for 10 min, 95°C for 15 s, 60°C for 1 min, and 72°C for 30 s, for a total of 40 cycles. The number of cycles at which fluorescent signals reach a detection threshold set within the exponential phase of the PCR reaction (C_t numbers) was used to calculate the expression levels of genes.

P450 enzyme assay using liquid chromatography-triple quadruple mass spectrometry

Vehicle (LLC-VEH) and lentiviral vector-transduced LLC-PK_1 cells (LLC-EGFP, LLC-Cyp4a10 and LLC-Cyp4a12) were harvested, and the proteins were extracted by homogenization and sonication. We initially used a tube homogenizer in a small volume (50 μl or less) to make sure that the cells were in close contact with the tube during this step. Afterward, we used a sonicator at a setting of 4 to break up the cells (3 × 5 s). Between the sonication steps, the cells were put on ice for 30 s to prevent excessive heat buildup. The supernatants were collected, proteins concentrations were measured, and 500 μg of protein was incubated in 0.1 M potassium phosphate buffer containing 2 mM NADPH and 40 μM cold arachidonic acid for a 0.5-ml total reaction volume. The reaction was incubated at 37°C and equilibrated with 100% O_2 for 30 min. The reaction was stopped by acidification to pH 3.5 with 1 M formic acid. The lipids were extracted in the presence of 20-HETE-d6 (2 ng) using 3:1 ethyl acetate:water and dried down under nitrogen. The samples were reconstituted in 1:1 methanol:water, and the production of 20-HETE was measured using a liquid chromatograph-triple quadruple mass spectrometer (ABI 3000, Applied Biosystems, Foster City, CA). To quantify the other metabolites of arachidonic acid in our assay, we ran a standard curve for each of the metabolites quantitated. Using the individual standards, each of the metabolites was identified based on retention time and fragmentation pattern. For the quantification, the abundance of each metabolite was calculated by using the peak area of the standards in the standard curve. As a normalization for the extraction efficiency of all of the metabolites, an internal standard (20-HETE-d6) was added during the extraction steps, and the peak value was multiplied by the percent recovery.

Experimental protocols

LLC-PK_1 cells were grown in α-MEM containing 10% FBS, 100 U/ml penicillin, and 100 μg/ml streptomycin, at 37°C in a 5% CO_2-95% air humidified incubator. For each of the experimental studies, the cells were grown to confluence in six-well plates before initiation of the injury (or substrate free) and recovery protocols. On the day of experiment, cells were washed with Dulbecco's PBS and incubated with prewarmed serum-free α-MEM 30 min before ATP depletion. ATP depletion was induced by substrate deprivation and the addition of 0.1 μM antimycin A, a complex III inhibitor, for 4 h (experimental protocol is detailed in Fig. 2). Substrate deprivation was achieved by not providing any amino acids or D-glucose in the injury media (IM). To maintain osmolarity, 5.5-mM nonmetabolizable form of glucose, L-glucose, was added. The IM consisted of (in mM) 5.5 L-glucose, 1× MEM vitamin solution (Invitrogen), 26 $NaHCO_3$, 5.4 KCl, 116 NaCl, 0.9 NaH_2PO_4 •$2H_2O$, 0.8 $MgSO_4$•$7H_2O$, 1.8 $CaCl_2$•$2H_2O$, and 0.0001 lipoic acid (Sigma). Following ATP depletion, media and cells were collected immediately (for ATP depletion alone, *time 4/0*) or recovered in serum-free α-MEM for an additional period of 2 h (for ATP depletion and recovery, *time 4/2*). The recovery media was serum-free α-MEM with 100 U/ml penicillin and 100 μg/ml streptomycin (Invitrogen). Control cells were grown in parallel and underwent equivalent

washes and incubated in serum-free α-MEM throughout the experiment. A subset of cells was transduced with GFP and Cyp4a12 constructs at a multiplicity of infection (MOI) of ~40 to examine the role of individual Cyp4a12 genes on ATP depletion/recovery. Additionally, LLC-EGFP cells (with and without ATP depletion) were treated with HET-0016 (10 μM), a selective inhibitor of 20-HETE synthesis. To test the role of superoxide in CYP4A-induced cytotoxicity, LLC-EGFP and LLC-Cyp4a12 cells were also treated with the cell-permeable SOD mimetic MnTMPyP (100 μM) 30 min before and during the ATP depletion/recovery periods (see Fig. 2). Unless otherwise stated, cells were lysed in RIPA lysis buffer with the addition of protease inhibitors. Protein concentration in cell lysates was measured using a protein assay kit from Bio-Rad (Hercules, CA).

Determination of cytotoxicity

The release of LDH into the media from normal (LLC-VEH) and lentiviral vector-transduced LLC-PK_1 cells (LLC-EGFP, LLC-Cyp4a10, and LLC-Cyp4a12) was measured using a commercially available kit (Diagnostic Chemicals, Oxford, CT) within 24 h of harvest. This kit is based on the conversion of L-lactate and NAD to pyruvate and NADH by the released LDH. The rate of increase in absorbance of the reaction mixture, from the formation of NADH, at 340 nm is proportional to the LDH activity.

Detection of superoxide formation

The production of superoxide in lentiviral vector-transduced LLC-PK_1 cells (LLC-EGFP, LLC-Cyp4a10, and LLC-Cyp4a12) following ischemic injury and recovery was determined qualitatively by dihydroethidium (DHE) fluorescence, a specific probe for intracellular $O_2^{\bullet-}$ production. For DHE fluorescence, LLC-EGFP and LLC-Cyp4a12 cells with and without MnTMPyP (100 μM) or HET-0016 (10 μM) were subjected to ATP depletion for 4 h followed by a 2-h recovery period (*time 4/2*) in serum-free media as outlined in the experimental protocols above (26). Cells were loaded with 10 μM hydroethidium (HE) 20 min before the end of the experiment. Cells were scanned for DHE red fluorescence using an Olympus IX50 inverted microscope (Olympus America, Center Valley, PA) equipped with rhodamine filter settings.

Detection of caspase-3 levels

The levels of caspase-3 (Upstate, Temecula, CA) were measured in the protein lysates harvested from the untreated (LLC-VEH) and lentiviral vector-transduced LLC-PK_1 cells (LLC-Cyp4a12) using a commercially available kit. This kit utilizes the detection of the chromophore *p*-nitroaniline (*p*NA), which was measured spectrophotometrically at 405 nm, after cleavage from labeled substrate *N*-acetyl-Asp-Glu-Val-Asp-pNA (DEVD-*p*NA). Released *p*NA was quantified by generating a *p*NA standard curve with caspase activity expressed as micromolar per minute per milligram protein. Western blot analysis for the activated caspase-3 was performed as another method to determine apoptosis. Ten micrograms of cellular protein was separated by 12% SDS-PAGE and transferred to nitrocellulose membrane for 1.5 h at 4°C. The membrane was blocked in LiCor blocking buffer (Lincoln, NE) and incubated with rabbit anti-caspase-3 (1:1,000, Cell Signaling, Danvers, MA) overnight at 4°C. Bound antibodies were incubated with IRDye infrared secondary antibodies (anti-rabbit IgG, 1:10,000, LiCor) for 1 h at room temperature and visualized with the use of the Odyssey Infrared Imaging System (LiCor).

Statistical analysis

Mean values ± SE are expressed. The significance of differences in mean values was evaluated by one-way ANOVA, followed by a Newman-Keuls multiple comparison test. $P < 0.05$ was considered statistically significant.

RESULTS

Validation of CYP4A expression and activity in genetically modified LLC-PK$_1$ cells using lentiviral vectors

LLC-PK$_1$ cells were serially transduced (MOI ~40) with various VSV-G pseudotyped lentiviral vectors expressing either the marker EGFP or CYP4A isoforms (Cyp4a10 and Cyp4a12) over a 4-day period to ensure that every cell was found to be genetically modified by the lentiviral vector. The LLC-PK$_1$ cells transduced with the EGFP marker were labeled as LLC-EGFP, and the Cyp4a10- and Cyp4a12-expressing cells were labeled LLC-Cyp4a10 and LLC-Cyp4a12, respectively. FACS analysis was performed on the LLC-EGFP cells, demonstrating extremely high transduction (>98%; $n = 3$ experiments) as shown in Fig. 1*A*. No EGFP fluorescence was detected in cells exposed to vehicle (LLC-VEH) or with the CYP4A isoforms (LLC-Cyp4a10 and LLC-Cyp4a12).

Steady-state levels of Cyp4a10 (Fig. 1*B*) and Cyp4a12 mRNA (Fig. 1*C*) were significantly increased as determined by RT-real-time PCR assay using SYBR green as the indicator. Specific primers were designed to minimize nonspecific amplification between the two nearly identical genetic sequences (Fig. 1, *B* and *C*) as shown by the significantly higher amplification of each product using their respective primers. The functional activity of the overexpressed CYP4A isoforms was determined by the P450 enzyme assay, which involves the metabolism of arachidonic acid and the breakdown products analyzed by liquid chromatography-quadruple mass spectroscopy. Total protein lysates isolated from the control (vehicle) LLC-VEH (Fig. 1*D*) demonstrated minimal 20-HETE production (0.02 ± 0.01 pmol•mg protein^{-1}•min^{-1}; $n = 3$), and no significant difference in 20-HETE production (0.03 ± 0.01 pmol•mg protein^{-1}•min^{-1}; $n = 3$) following transduction with the EGFP-expressing lentiviral vectors (LLC-EGFP). Significantly higher ($P < 0.05$) production of 20-HETE was observed in LLC-Cyp4a10 (2.25 ± 0.13 pmol•mg protein^{-1}•min^{-1}; $n = 3$) and LLC-Cyp4a12 (3.74 ± 0.93 pmol•mg protein^{-1}•min^{-1}; $n = 3$), and the production of 20-HETE (0.01 ± 0.00 pmol•mg protein^{-1}•min^{-1}; $n = 3$) could be selectively blocked using HET-0016 at a dose of 1 μM. Western blot analysis of LLC-Cyp4a10 and LLC-Cyp4a12 protein lysates demonstrated markedly higher levels of CYP4A protein compared with the LLC-EGFP or LLC-VEH cells (data not shown), which was consistent with the functional P450 enzyme assay.

Figure 1*E* demonstrated that none of the other HETE or EET molecules were markedly different among the LLC-EGFP, LLC-Cyp4a10, or LLC-Cyp4a12 cells other than the lower production of 5-HETE in LLC-Cyp4a12 cells. Since both LLC-Cyp4a10 and LLC-Cyp4a12 cells were able to overexpress 20-HETE, we focused the remainder of our study on Cyp4a12-mediated 20-HETE overproduction in the context of IR injury in the renal epithelial cell culture model.

Determination of cytotoxicity in LLC-Cyp4a12 cells following ATP depletion and recovery

As illustrated in Fig. 2, the basic protocol that we used in our study was to incubate the LLC-PK$_1$ cells transduced with lentiviral vector variants for a period of 4 h in normal (serum-free) or IM, and the cells and media were either directly analyzed after this period (denoted as *time 4/0*) or after an additional 2-h recovery period in normal serum-free media (denoted as *time 4/2*). The IM consisted of (in mM) 5.5 L-glucose, 1× MEM vitamin solution (Invitrogen), 26 $NaHCO_3$, 5.4 KCl, 116 NaCl, 0.9 NaH_2PO_4•$2H_2O$, 0.8 $MgSO_4$•$7H_2O$, 1.8 $CaCl_2$•$2H_2O$, and 0.0001 lipoic acid (Sigma) with the addition of 0.1 μM antimycin A, a complex II inhibitor. Using this approach (Fig. 3*A*), we detected a slight increase in the LDH levels in LLC-EGFP cells at *time 4/0* (2.89 ± 0.22 mU/mg protein, $n = 9$) and *4/2* (2.92 ± 0.11 mU/mg protein, $n = 6$) compared with the serum-free controls at *time 4/0* (1.88 ± 0.24

mU/mg protein, $n = 9$) and *4/2* (2.14 ± 0.19 mU/mg protein, $n = 9$). No significant change was detected in LDH levels when LLC-Cyp4a12 cells were compared with LLC-EGFP cells at *time 4/0* (Fig. 3*A*), but there was a significant increase in LDH levels at *time 4/2* in LLC-Cyp4a12 cells (5.95 ± 1.03 mU/mg protein, $n = 9$) vs. serum-free time control (2.36 ± 0.33 mU/mg protein, $n = 8$, $P < 0.01$) or with LLC-EGFP cells (2.92 ± 0.11, $n = 6$, $P < 0.05$). No significant change in LDH levels was observed when LLC-Cyp4a12 and LLC-EGFP cells incubated in the serum-free media throughout the experiment were compared.

Treatment with HET-0016 did not have any effect on LDH release in LLC-Cyp4a12 cells immediately after the ATP depletion time period (*time 4/0*; Fig. 3*A*). After an additional 2 h of recovery in the serum-free media (*time 4/2*) in the presence of HET-0016 (10 μM), LDH levels in LLC-Cyp4a12 cells were significantly lower ($P < 0.05$) than that seen in the control cells and was reduced from 5.95 ± 1.03 to 3.8 ± 0.29 mU/mg protein ($n = 9$).

To examine the role of $O_2^{\bullet -}$ as a potential mediator leading to the increased release of LDH following 20-HETE production, we pretreated LLC-Cyp4a12 cells with a cell-permeable SOD mimetic, MnTMPyP, at a dose of 100 μM. This resulted in a small, but nonsignificant decrease to 4.29 ± 0.86 ($n = 6$) compared with the nontreated LLC-Cyp4a12 cells at *time 4/2* (5.95 ± 1.03 mU/mg protein, $n = 9$). No significant change using LLC-EGFP cells with respect to the release of LDH was noted in the presence or absence of MnTMPyP at either *time 4/0* or *4/2* (Fig. 3*B*).

Role of superoxides in LLC-cyp4a12 cells following ATP depletion and recovery

Qualitative assessment of superoxide formation was made using a DHE oxidation assay on live LLC-PK_1 cells transduced with the lentiviral vector variants. DHE fluorescence showed an increase in superoxide levels to the same degree in LLC-EGFP or LLC-Cyp4a12 cells (Fig. 4*A*, *left* panel) at *time 4/2*, and the treatment with HET-0016 (10 μM) did not markedly affect the intensity of DHE fluorescence.

In the presence of the SOD mimetic MnTMPyP (100 μM) there was a tremendous reduction in DHE fluorescence compared with LLC-Cyp4a12 cells incubated in ischemic conditions in the absence of the mimetic. This was indicative of active scavenging of the free radicals by MnTMPyP to make the DHE fluorescence similar to the LLC-Cyp4a12 cells incubated in control (serum-free) conditions (Fig. 4*B*).

Role of caspase-3 in mediating apoptosis in LLC-cyp4a12 cells following ATP depletion and recovery

To assess whether the increased cytotoxicity in the LLC-Cyp4a12 cells was associated with apoptosis, we examined the changes in caspase-3 levels, which is an index of apoptosis, following 4-h ischemic and subsequent 2-h recovery periods (*time 4/2*) between control LLC-EGFP and experimental LLC-Cyp4a12 cells. Following *time 4/2*, no significant change in caspase-3 levels was detected between the ischemic (ATP-depleted media) and non-ischemic (serum-free media) conditions in LLC-EGFP cells (Fig. 5*A*). However, LLC-Cyp4a12 cells incubated in ATP-depleted media (40.65 ± 7.10 μM•min^{-1}•mg $protein^{-1}$, $n = 6$, $P < 0.01$) exhibited a 2-fold increase in the level of activated caspase-3 compared with LLC-EGFP (20.74 ± 4.48 μM•min−1 •mg $protein^{-1}$, $n = 3$) cells in ATP-depleted media and a 10-fold increase compared with control (serum-free) media (4.17 ± 2.09 μM•min^{-1} •mg $protein^{-1}$, $n = 3$). Blockade of 20-HETE synthesis with 10 μM HET-0016 (16.30 ± 4.10 μM•min^{-1} •mg $protein^{-1}$, $n = 3$, $P < 0.05$) during the injury and recovery periods in LLC-Cyp4a12 cells resulted in a significant decrease in the caspase-3 levels compared with the untreated LLC-Cyp4a12 cells (Fig. 5*A*).

To determine the role of free radicals on mediating apoptosis through caspase-3 in LLC-Cyp4a12 cells, we treated the cells with vehicle or a SOD mimetic, MnTMPyP (100 μM), during the ischemic and recovery periods (Fig. 5*A*). In the presence of MnTMPyP (13.78 ± 3.28 $\mu M \bullet min^{-1} \bullet mg\ protein^{-1}$, $n = 6$), there was a significant reduction ($P < 0.05$) in the caspase- 3 levels compared with the untreated, ATP-depleted LLC-Cyp4a12 cells (40.65 ± 7.10 $\mu M \bullet min^{-1} \bullet mg\ protein^{-1}$, $n = 6$).

By Western blot analysis, we confirmed our results that caspase-3 played a role in the cytotoxicity associated with the cells by using a specific antibody that recognized the activated products of caspase-3 (17- and 20-kDa bands). In Fig. 5*B*, we found that the activated caspase-3 bands (17- and 20-kDa) in the LLC-Cyp4a12 incubated in ischemic conditions were markedly higher than the control (serum-free) cells at *time 4/2*. Moreover, we found that there was a decrease in the activated caspase-3 band intensities at 17 and 20 kDa in the presence of HET-0016. No significant difference was noted in LLC-EGFP cells in caspase-3 levels in the different conditions.

DISCUSSION

The present study examined the effects of 20-HETE production on an in vitro model of IR injury using LLC-PK_1 cells. Although freshly isolated renal tubular epithelial cells as well as hepatocytes avidly express CYP450 enzymes, it has been well characterized that the expression and function of CYP450 are rapidly lost in culture. This is partially due to the rapid inactivation of CYP450 by the binding of nitric oxide (NO) and carbon monoxide (CO) produced by these proliferating cells, which targets these NO- or CO-bound enzymes for degradation (6,43,45).

Characterization of lentiviral vector-modified LLC-PK_1 cells

Incubation of LLC-PK_1 cells in an ATP-depleted media has been previously shown to be an acceptable in vitro model to study IR injury (40). Since these cells do not normally produce 20-HETE, we overcame this obstacle by genetically modifying LLC-PK_1 renal epithelial cells using lentiviral vectors expressing CYP4504A isoforms. This method was capable of restoring the ability of these cells to produce 20-HETE like normal proximal tubule epithelial cells. Using traditional transfection methods with naked DNA generally results in extremely low efficiencies in the ability to modify LLC-PK_1 cells and requires laborious and time-consuming selection to obtain clonal populations. The use of VSV-G pseudotyped replication-defective lentiviral vectors was found to be extremely effective in transducing LLC-PK_1 cells with either the marker gene, EGFP, or our transgenes of interest, murine Cyp4a10 and Cyp4a12, which are homologs of rodent CYP4A1 and CYP4A8, respectively. The advantage in using lentiviral vectors is their innate ability to integrate into the host genome, allowing for long-term, stable transgene expression, and the expression of the integrated transgene can be propagated in successive passages. This is unlike other currently available viral vectors, which infect cells and remain predominantly episomal, so propagation of vector-transduced cells would lead to a rapid loss of the vector particle and its associated ability to express the transgene.

The lentiviral vector-transduced LLC-PK_1 cells with the Cyp4a10 or Cyp4a12 were capable of specifically producing 20-HETE compared with the LLC-EGFP cells, which remained unable to produce 20-HETE. Moreover, there was minimal change in the other arachidonic acid breakdown products, including other variants of HETEs, diHETEs, and EETs, following the expression of the CYP4A isoforms in the LLC-PK_1 cells. These experiments demonstrate the efficiency and speed in using lentiviral vectors to manipulate the expression of transgenes in LLC-PK_1 cells to study the effects of 20- HETE in IR injury.

Effect of overexpression of Cyp4a12 on LLC-PK$_1$ cells following ATP depletion and recovery

Using the lentiviral vector-transduced LLC-PK$_1$ cells to overexpress CYP4A iso-forms, we found that 20-HETE production exacerbated the cytotoxicity following an ATP depletion step for 4 h followed by a 2-h recovery period (*time 4/2*). In contrast, time course experiments using ATP depletion for 2 h alone (*time 2/0*) or followed by a 2-h recovery period in serum-free media (*time 2/2*) did not show any significant increase in cytotoxicity as determined by LDH release using LLC-EGFP and LLC-Cyp4a12 cells compared with their serum-free time control cells (unpublished observations). This was not surprising, because we qualitatively observed that the 2-h ischemia only caused the cells to appear more "stressed" but that the cells would remain adhered to the plates without undergoing a typical cell death, as observed using the 4-h ATP depletion step. For this reason, we focused our experiments using the longer 4-h ATP depletion period with and without a 2-h recovery phase for the remainder of our studies.

Following 4 h of ATP depletion and recovery, cytotoxicity was significantly higher in LLC-Cyp4a12 cells producing 20-HETE compared with LLC-EGFP cells, which was blocked following inhibition with a specific inhibitor of CYP4A, HET- 0016. It is important to note that the increased release in LDH, which is the marker for cytotoxicity, following *time 4/2* is similar to the increase observed in naïve LLC-PK$_1$ cells incubated in ATP-depleted conditions for longer than 6 h (unpublished observations). These findings suggest a destructive role for 20-HETE to not only exacerbate but possibly accelerate the cell death associated with the simulated IR injury. These effects were not specific only to the overexpression of Cyp4a12, since similar cytotoxic effects were found using LLC-Cyp4a10 cells (data not shown).

There is a paucity of studies documenting the role of 20-HETE as a negative mediator in the kidney following IR injury. However, our in vitro findings demonstrating the protective effects of blocking CYP4A ω-hydroxylase activity using HET-0016 in the LLC-PK$_1$ cells during the recovery (or reperfusion) phase of the experiment is consistent with the in vivo findings in dog hearts following IR injury in the presence of 17-ODYA or a 20-HETE antagonist, 20-HEDE (27). The mechanism by which HET-0016 exerts its protective effects on renal epithelial cells remains to be determined. One possible explanation may involve a deleterious interaction by 20-HETE with newly formed reactive oxygen species during the recovery phase. It has been well established that a rapid and large burst of reactive oxygen species can be produced through the actions of xanthine oxidase (19,20) and NADPH oxidase (4) during the reperfusion step following an ischemic episode. The synergistic interaction with 20-HETE and superoxides was also found in a previous study by Guo et al. (8), who found that these molecules worked together to enhance endothelial cell proliferation through a p42/p44 MAPK-dependent pathway. Since CYP4A overexpression increased cytotoxicity primarily in the recovery phase in the LLC-PK$_1$ cells after ATP depletion, we explored the possibility of whether superoxide played a role in potentiating the increased cytotoxicity associated with 20-HETE production. In the presence of the SOD mimetic MnTMPyP, we found that the cytotoxic effects of 20-HETE production was not significantly attenuated, indicating that the deleterious effects of 20-HETE production were not completely dependent on superoxide. It is possible that 20-HETE may be exerting its cytotoxic effects via the actions of other free radical species such as the hydroxyl radical. Although we have not measured this directly in this study, there are reports that suggest that CYP450 metabolites mediate tissue damage via the hydroxyl radical during reoxygenation injury in the kidney (29).

Ultimately, the continual production of 20-HETE following ATP depletion and recovery resulted in increased cell death, in part due to the activation of caspase-3-mediated

apoptosis. This is consistent with previous studies demonstrating the importance of apoptotic signaling pathways in mediating cell death in renal IR injury (3,7,17,18), and these pathways converge on the effector protease of apoptosis, caspase-3. The increased activity of caspase-3 was blocked by the SOD mimetic MnTMPyP and the inhibitor to 20-HETE synthesis HET-0016. There was a concomitant decrease in caspase-3 activity found using LLC-EGFP cells treated with HET-0016, and this may indicate that low levels of 20-HETE normally produced in LLC-PK_1 cells may be involved in the basal activity of caspase-3 activation. However, high levels of 20- HETE stimulated caspase-3 activation, as shown by using LLC-4a12 cells. In the presence of HET-0016, caspase-3 activation in LLC-4a12 cells only returned 20-HETE production down to levels detected under serum-free conditions, so it may be possible that the blockade was not complete and that there is sufficient 20-HETE synthesis leading to the higher caspase-3 activity compared with LLC-EGFP cells. Alternatively, there are many regulatory steps that lead to the activation of caspase-3, and it may be possible that a non-20-HETE-mediated factor was blocked, leading to the increased cleavage of caspase-3. These results show that 20-HETE may play a role in mediating a proapoptotic effect in renal epithelial cells during the recovery phase following an ischemic episode, but the mechanism remains to be fully elucidated. There are several possible mechanisms by which 20-HETE inhibition may provide renal cell protection following IR injury. One mechanism may be the activation of K*ATP* channels similar to the findings in the heart (36) following 20-HETE blockade. Another possibility may be the involvement of 20-HETE in stimulating the activation of PKB (or Akt), which mediates the phosphorylation of eNOS, leading to decreased interaction with heat shock protein 90 (1). In the latter possibility, this mechanism was found to activate caspase-3 in bovine pulmonary endothelial cells (1). Further studies are warranted to determine the complex interaction between 20-HETE with superoxides and the signal transduction pathways activated to mediate cytotoxicity in IR injury in the kidney.

In conclusion, the present study demonstrated that continual production of 20-HETE increases cytotoxicity in porcine renal epithelial LLC-PK_1 cells following a simulated IR injury model. The increased cell death is associated with increased caspase-3 levels, which can be blocked by a specific inhibitor of 20-HETE synthesis, HET-0016, and a superoxide scavenger, MnTMPyP. This suggests that 20-HETE mediates the proapoptotic effects on the renal epithelial cells during the recovery phase following an ischemic episode partially through a superoxide-dependent pathway. These results suggest that enhanced release of 20-HETE following IR injury contributes to the cellular damage and death and that inhibitors of the CYP4A family may be therapeutically useful in the protection of the kidney from IR injury.

Acknowledgments

The authors thank Averia Steinman and Katherine Friedrich for technical help with the liquid chromatography-quadruple mass spectroscopy to measure 20-HETE production.

GRANTS

This work was funded in part by an American Heart Association Beginning Grant-In-Aid (F. Park.), departmental funds (V. Nilakantan), and National Heart, Lung, and Blood Institute Grant HL 36279 (R. J. Roman).

REFERENCES

1. Chen Y, Medhora M, Falck JR, Pritchard KA Jr, Jacobs ER. Mechanisms of activation of eNOS by 20-HETE and VEGF in bovine pulmonary artery endothelial cells. Am J Physiol Lung Cell Mol Physiol. 2006; 291:L378–L385. [PubMed: 16679377]

2. Chien CT, Hsu SM, Chen CF, Lee PH, Lai MK. Prolonged ischemia potentiates apoptosis formation during reperfusion by increase of caspase 3 activity and free radical generation. Transplant Proc. 2000; 32:2065–2066. [PubMed: 11120068]
3. Dagher PC. Apoptosis in ischemic renal injury: roles of GTP depletion and p53. Kidney Int. 2004; 66:506–509. [PubMed: 15253698]
4. Dodd OJ, Pearse DB. Effect of the NADPH oxidase inhibitor apocyanin on ischemia-reperfusion lung injury. Am J Physiol Heart Circ Physiol. 2000; 279:H303–H312. [PubMed: 10899070]
5. Dull T, Zufferey R, Kelly M, Mandel RJ, Nguyen M, Trono D, Naldini L. A third-generation lentivirus vector with a conditional packaging system. J Virol. 1998; 72:8463–8471. [PubMed: 9765382]
6. Eum HA, Yeom DH, Lee SM. Role of nitric oxide in the inhibition of liver cytochrome P450 during sepsis. Nitric Oxide. 2006; 15:423–431. [PubMed: 16884934]
7. Feldenberg LR, Thevananther S, del Rio M, de Leon M, Devarajan P. Partial ATP depletion induces Fas- and caspase-mediated apoptosis in MDCK cells. Am J Physiol Renal Physiol. 1999; 276:F837–F846.
8. Guo AM, Arbab AS, Falck JR, Chen P, Edwards PA, Roman RJ, Scicli AG. Activation of vascular endothelial growth factor through reactive oxygen species mediates 20-hydroxyeicosatetraenoic acid-induced endothelial cell proliferation. J Pharmacol Exp Ther. 2007; 321:18–27. [PubMed: 17210799]
9. Imig JD, Zou AP, Stec DE, Harder DR, Falck JR, Roman RJ. Formation and actions of 20-hydroxyeicosatetraenoic acid in rat renal arterioles. Am J Physiol Regul Integr Comp Physiol. 1996; 270:R217–R227.
10. Ito O, Alonso-Galicia M, Hopp KA, Roman RJ. Localization of cytochrome P-450 4A isoforms along the rat nephron. Am J Physiol Renal Physiol. 1998; 274:F395–F404.
11. Ito O, Omata K, Ito S, Hoagland KM, Roman RJ. Effects of converting enzyme inhibitors on renal P-450 metabolism of arachidonic acid. Am J Physiol Regul Integr Comp Physiol. 2001; 280:R822–R830. [PubMed: 11171663]
12. Ito O, Roman RJ. Regulation of *P*-450 4A activity in the glomerulus of the rat. Am J Physiol Regul Integr Comp Physiol. 1999; 276:R1749–R1757.
13. Ito O, Roman RJ. Role of 20-HETE in elevating chloride transport in the thick ascending limb of Dahl SS/Jr rats. Hypertension. 1999; 33:419–423. [PubMed: 9931140]
14. Kaushal GP, Ueda N, Shah SV. Role of caspases (ICE/CED 3 proteases) in DNA damage and cell death in response to a mitochondrial inhibitor, antimycin A. Kidney Int. 1997; 52:438–445. [PubMed: 9263999]
15. Kellerman PS, Bogusky RT. Microfilament disruption occurs very early in ischemic proximal tubule cell injury. Kidney Int. 1992; 42:896–902. [PubMed: 1453583]
16. Kellerman PS, Clark RA, Hoilien CA, Linas SL, Molitoris BA. Role of microfilaments in maintenance of proximal tubule structural and functional integrity. Am J Physiol Renal Fluid Electrolyte Physiol. 1990; 259:F279–F285.
17. Lieberthal W, Koh JS, Levine JS. Necrosis and apoptosis in acute renal failure. Semin Nephrol. 1998; 18:505–518. [PubMed: 9754603]
18. Lieberthal W, Levine JS. Mechanisms of apoptosis and its potential role in renal tubular epithelial cell injury. Am J Physiol Renal Fluid Electrolyte Physiol. 1996; 271:F477–F488.
19. McCord JM, Roy RS. The pathophysiology of superoxide: roles in inflammation and ischemia. Can J Physiol Pharmacol. 1982; 60:1346–1352. [PubMed: 6295573]
20. McCord JM, Roy RS, Schaffer SW. Free radicals and myocardial ischemia. The role of xanthine oxidase. Adv Myocardiol. 1985; 5:183–189. [PubMed: 2982206]
21. Miyata N, Roman RJ. Role of 20-hydroxyeicosatetraenoic acid (20-HETE) in vascular system. J Smooth Muscle Res. 2005; 41:175–193. [PubMed: 16258232]
22. Miyata N, Seki T, Tanaka Y, Omura T, Taniguchi K, Doi M, Bandou K, Kametani S, Sato M, Okuyama S, Cambj-Sapunar L, Harder DR, Roman RJ. Beneficial effects of a new 20-hydroxyeicosatetraenoic acid synthesis inhibitor, TS-011 [*N*-(3-chloro-4-morpholin-4-yl) phenyl-*N*′-hydroxyimido formamide], on hemorrhagic and ischemic stroke. J Pharmacol Exp Ther. 2005; 314:77–85. [PubMed: 15831442]

23. Molitoris BA. New insights into the cell biology of ischemic acute renal failure. J Am Soc Nephrol. 1991; 1:1263–1270. [PubMed: 1912388]
24. Moreno C, Maier KG, Hoagland KM, Yu M, Roman RJ. Abnormal pressure-natriuresis in hypertension: role of cytochrome P450 metabolites of arachidonic acid. Am J Hypertens. 2001; 14:90S–97S. [PubMed: 11411771]
25. Naldini L, Blomer U, Gage FH, Trono D, Verma IM. Efficient transfer, integration, and sustained long-term expression of the transgene in adult rat brains injected with a lentiviral vector. Proc Natl Acad Sci USA. 1996; 93:11382–11388. [PubMed: 8876144]
26. Nilakantan V, Zhou X, Hilton G, Shi Y, Baker JE, Khanna AK, Pieper GM. Antagonizing reactive oxygen by treatment with a manganese (III) metalloporphyrin-based superoxide dismutase mimetic in cardiac transplants. J Thorac Cardiovasc Surg. 2006; 131:898–906. [PubMed: 16580450]
27. Nithipatikom K, Gross ER, Endsley MP, Moore JM, Isbell MA, Falck JR, Campbell WB, Gross GJ. Inhibition of cytochrome P450omega-hydroxylase: a novel endogenous cardioprotective pathway. Circ Res. 2004; 95:e65–e71. [PubMed: 15388642]
28. Omura T, Tanaka Y, Miyata N, Koizumi C, Sakurai T, Fukasawa M, Hachiuma K, Minagawa T, Susumu T, Yoshida S, Nakaike S, Okuyama S, Harder DR, Roman RJ. Effect of a new inhibitor of the synthesis of 20-HETE on cerebral ischemia reperfusion injury. Stroke. 2006; 37:1307–1313. [PubMed: 16601220]
29. Paller MS, Jacob HS. Cytochrome P-450 mediates tissue-damaging hydroxyl radical formation during reoxygenation of the kidney. Proc Natl Acad Sci USA. 1994; 91:7002–7006. [PubMed: 8041736]
30. Park F. Correction of bleeding diathesis without liver toxicity using arenaviral-pseudotyped HIV-1-based vectors in hemophilia A mice. Hum Gene Ther. 2003; 14:1489–1494. [PubMed: 14577928]
31. Park F, Ohashi K, Chiu W, Naldini L, Kay MA. Efficient lentiviral transduction of liver requires cell cycling in vivo. Nat Genet. 2000; 24:49–52. [PubMed: 10615126]
32. Park F, Ohashi K, Kay MA. The effect of age on hepatic gene transfer with self-inactivating lentiviral vectors in vivo. Mol Ther. 2003; 8:314–323. [PubMed: 12907154]
33. Qian Z, Haessler M, Lemos JA, Arsenault JR, Aguirre JE, Gilbert JR, Bowler RP, Park F. Targeting vascular injury using Hantavirus-pseudotyped lentiviral vectors. Mol Ther. 2006; 13:694–704. [PubMed: 16431160]
34. Quigley R, Baum M, Reddy KM, Griener JC, Falck JR. Effects of 20-HETE and 19(*S*)-HETE on rabbit proximal straight tubule volume transport. Am J Physiol Renal Physiol. 2000; 278:F949–F953. [PubMed: 10836982]
35. Seki T, Ishimoto T, Sakurai T, Yasuda Y, Taniguchi K, Doi M, Sato M, Roman RJ, Miyata N. Increased excretion of urinary 20-HETE in rats with cyclosporine-induced nephrotoxicity. J Pharmacol Sci. 2005; 97:132–137. [PubMed: 15655287]
36. Seubert JM, Zeldin DC, Nithipatikom K, Gross GJ. Role of epoxyeicosatrienoic acids in protecting the myocardium following ischemia/reperfusion injury. Prostaglandins Other Lipid Mediat. 2007; 82:50–59. [PubMed: 17164132]
37. Stec DE, Flasch A, Roman RJ, White JA. Distribution of cytochrome *P*-450 4A and 4F isoforms along the nephron in mice. Am J Physiol Renal Physiol. 2003; 284:F95–F102. [PubMed: 12388424]
38. Takeuchi K, Renic M, Bohman QC, Harder DR, Miyata N, Roman RJ. Reversal of delayed vasospasm by an inhibitor of the synthesis of 20-HETE. Am J Physiol Heart Circ Physiol. 2005; 289:H2203–H2211. [PubMed: 15964920]
39. Tamura Y, Imaoka S, Gemba M, Funae Y. Effects of ischemia-reperfusion on individual cytochrome P450 isoforms in the rat kidney. Life Sci. 1997; 60:143–149. [PubMed: 9000120]
40. Van Why SK, Mann AS, Ardito T, Thulin G, Ferris S, Macleod MA, Kashgarian M, Siegel NJ. Hsp27 associates with actin and limits injury in energy depleted renal epithelia. J Am Soc Nephrol. 2003; 14:98–106. [PubMed: 12506142]

41. Venkatachalam MA, Jones DB, Rennke HG, Sandstrom D, Patel Y. Mechanism of proximal tubule brush border loss and regeneration following mild renal ischemia. Lab Invest. 1981; 45:355–365. [PubMed: 7300248]

42. Wang H, Garvin JL, Falck JR, Ren Y, Sankey SS, Carretero OA. Glomerular cytochrome P-450 and cyclooxygenase metabolites regulate efferent arteriole resistance. Hypertension. 2005; 46:1175–1179. [PubMed: 16230518]

43. Wang MH, Wang J, Chang HH, Zand BA, Jiang M, Nasjletti A, Laniado-Schwartzman M. Regulation of renal CYP4A expression and 20-HETE synthesis by nitric oxide in pregnant rats. Am J Physiol Renal Physiol. 2003; 285:F295–F302. [PubMed: 12684227]

44. Ward NC, Puddey IB, Hodgson JM, Beilin LJ, Croft KD. Urinary 20-hydroxyeicosatetraenoic acid excretion is associated with oxidative stress in hypertensive subjects. Free Radic Biol Med. 2005; 38:1032–1036. [PubMed: 15780761]

45. Watabe M, Isogai Y, Numazawa S, Yoshida T. Role of c-Myc in nitric oxide-mediated suppression of cytochrome P450 3A4. Life Sci. 2003; 74:99–108. [PubMed: 14575816]

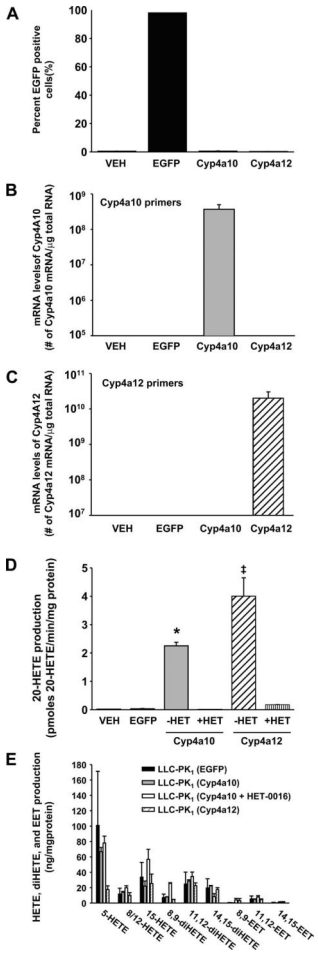

Fig. 1.

Genetic modification of LLC-PK_1 cells using lentiviral vectors. Vesicular stomatitis virus G (VSV-G) pseudotyped lentiviral vectors [multiplicity of infection (MOI) 40] were used to transduced LLC-PK_1 cells to overexpress green fluorescent protein (EGFP) and cytochrome *P*-450 4a10 (Cyp4a10) and -4a12 (Cypa12). *A*: graph showing the EGFP-expressing LLC-PK_1 cells following transduction with lentiviral vectors expressing EGFP (filled bars), Cyp4a10 (grey bar), and Cyp4a12 (hatched bars) compared with vehicle-treated cells (VEH; dots). *B* and *C*: graph of the steady-state levels of Cyp4a10 (*B*) and Cyp4a12 mRNA (*C*) using specific primers in RT-real-time PCR. *D*: 20-HETE production in LLC-PK_1 cells following transduction with the various lentiviral vectors in the presence (+HET) and absence (−HET) of the 20-HETE synthesis inhibitor HET-0016 (1 μM). *E*: production of alternative structures of HETE, diHETE, and EET following transduction with EGFP (filled bars), Cyp4a10 (grey bars), Cyp4a10 in the presence of HET-0016 (1 μM; stippled bars), and Cyp4a12 (hatched bars), and Cyp4a12 in the presence of HET-0016 (1 μM, vertical bars); $n = 3–5$ different experiments/sample, $^*P < 0.05$ Cyp4a10 vs. VEH and Cyp4a10+HET. ‡$P < 0.001$ Cyp4a12 vs. VEH and Cyp4a12.

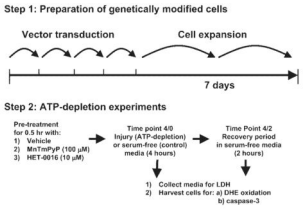

Fig. 2.

Experimental protocol. Schematic diagram of the ATP depletion and recovery protocols. Lentiviral vector-transduced cells were incubated for 4 h in serum-free or injury media at which point the experiment was ended (denoted as *time 4/0*) or an additional 2-h recovery period was performed in serum-free media before the completion of the experiment (denoted as *time 4/2*).

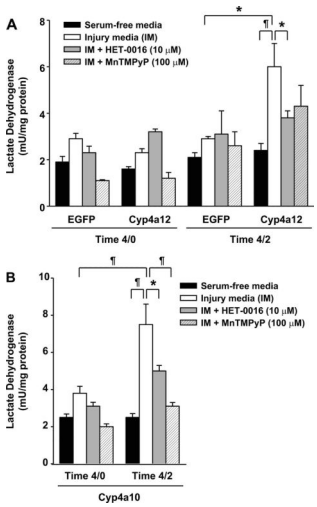

Fig. 3.

Role of cytochrome *P*-450 4a12 (Cyp4a12) on cytotoxicity. Cytotoxicity was assayed by measuring the lactate dehydrogenase (LDH) secreted into the media following the ATP depletion alone (*time 4/0*) or ATP depletion and recovery periods (*time 4/2*). *A*: effect of 20-HETE inhibition by HET-0016 (10 μM) on cytotoxicity following ATP depletion (*time 4/0*) or ATP depletion and recovery (*time 4/2*) in LLC-PK_1 cells. *B*: effect of the SOD mimetic MnTmPyP (100 μM) on cytotoxicity following ATP depletion (*time 4/0*) or ATP depletion and recovery (*time 4/2*) in LLC-PK_1 cells. S, serum-free controls; IM, injury media; IM+M, injury media+MnTmPyP; IM+H, injury media+HET- 0016. Values are means ± SE. ‡$P <$ 0.001. ¶ $P < 0.01$. *$P < 0.05$; n 5–12 for all groups.

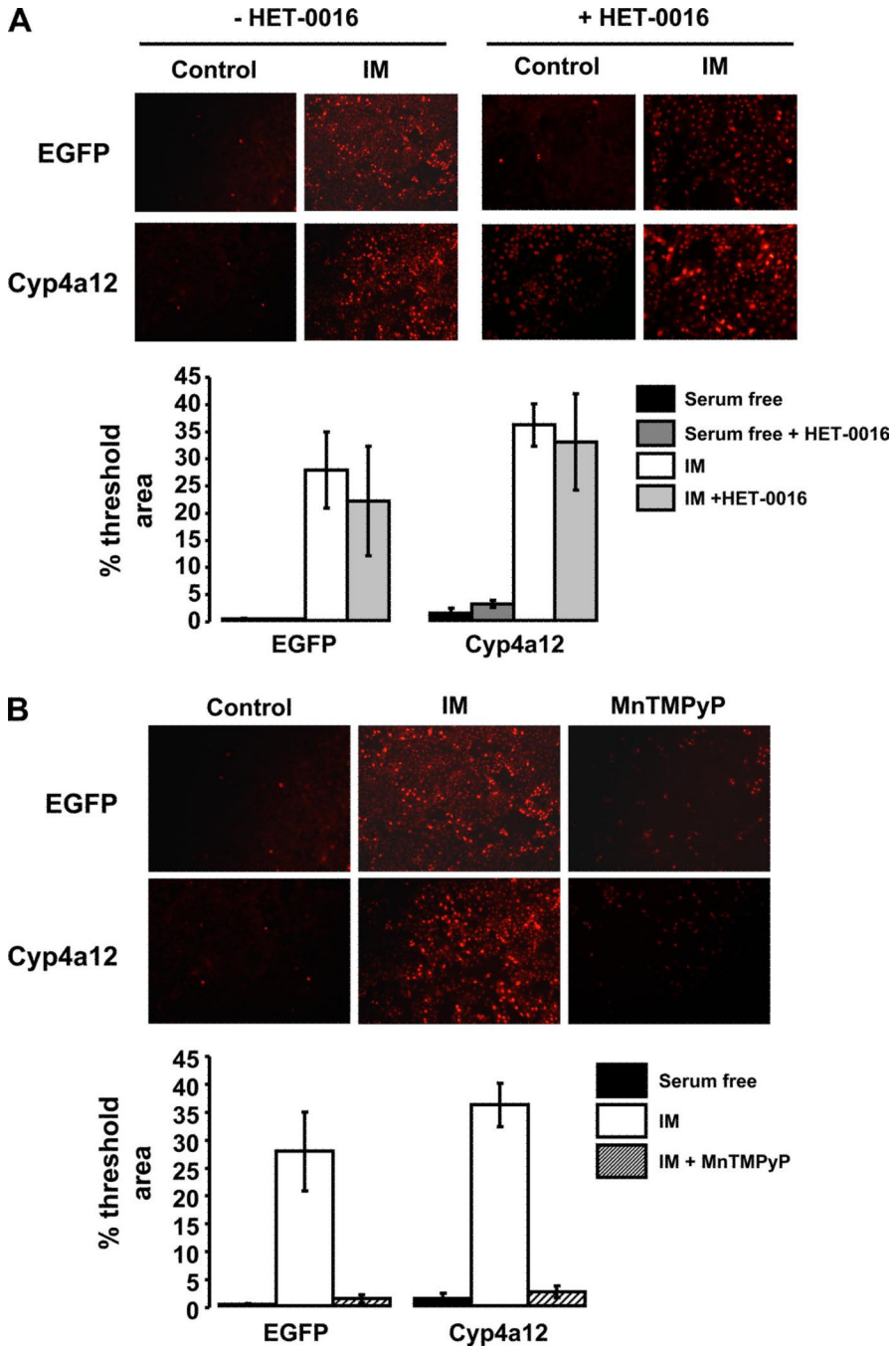

Fig. 4.

Role of Cyp4a12 on dihydroethidium (DHE) fluorescence. DHE fluorescence microscopic images showing intracellular superoxide production in LLC-EGFP and LLC-4a12 cells following ATP depletion and recovery (*time 4/2*). *A*: DHE fluorescence microscopic images showing intracellular superoxide production in the absence of HET-0016 (*left*) and in the presence of HET-0016 (*right*) in LLC-EGFP and LLC-Cyp4a12 cells following ATP depletion and recovery (*time 4/2*). Images are representative of 3 separate experiments. *B*: DHE fluorescence microscopic images showing effect of MnTmPyP (100 μM) on superoxide production in LLC-EGFP and LLC-Cyp4a12 cells following ATP depletion and recovery (*time 4/2*). Images are representative of 3 separate experiments.

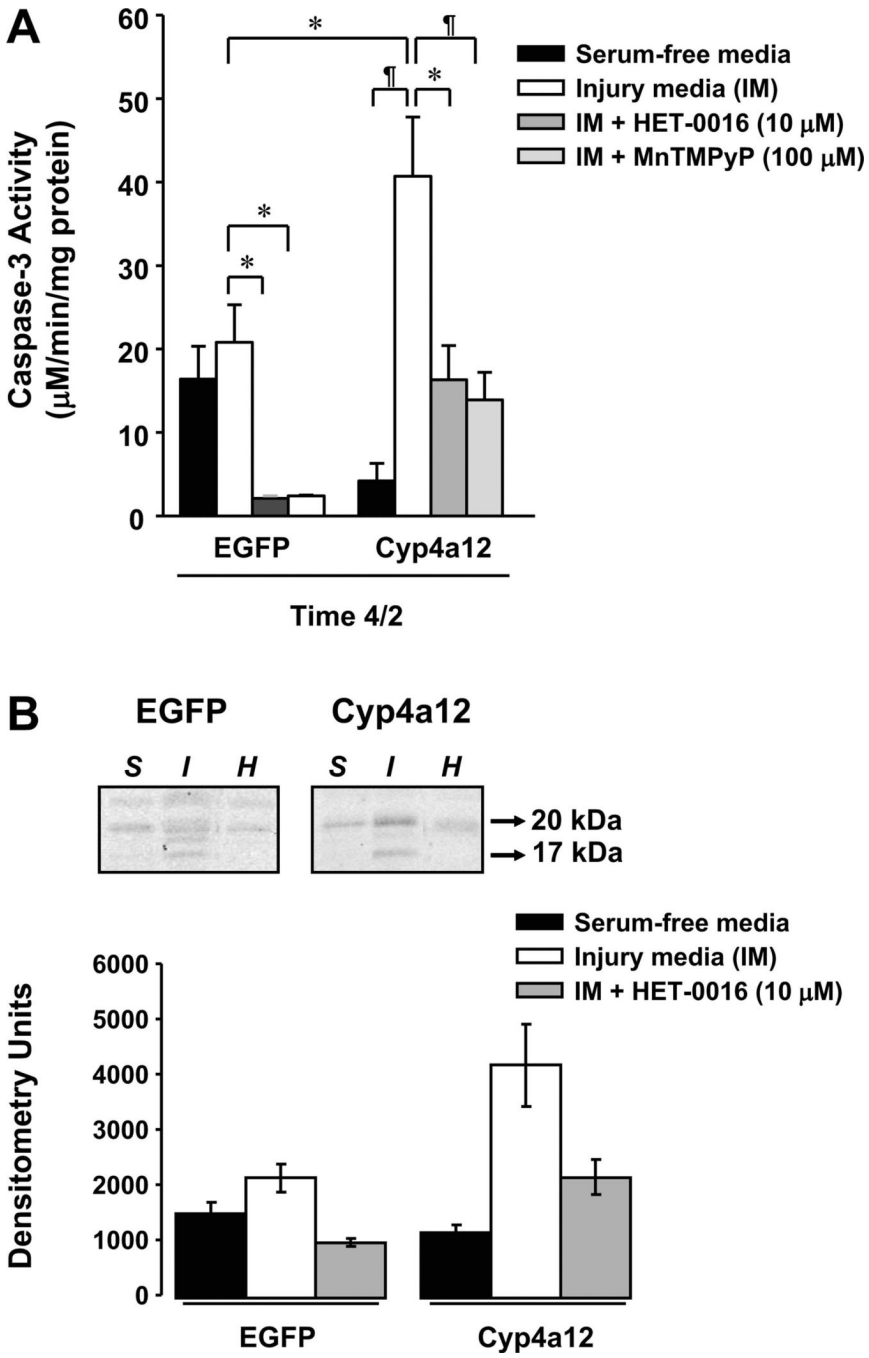

Fig. 5.

Role of Cyp4a isoforms on caspase-3 activity. *A*: effect of the SOD mimetic MnTMPyP (100 μM) and 20-HETE inhibitor HET-0016 (10 μM) on caspase-3 activity in EGFP and Cyp4a12-transduced cells following ATP depletion and recovery (*time 4/2*). *B*: Western blot showing effect of HET-0016 (10 μM) on activated caspase-3 (17 and 20 kDa) in EGFP and Cyp4a12-transduced cells following ATP depletion and recovery (*time 4/2*). Blot is representative of 3 individual samples. Abbreviations are defined as in Fig. 3. Values are means ± SE. ¶$P < 0.01$. *$P < 0.05$; $n = 3–6$.